

Gravitational Wave Spectra from Primordial Magnetohydrodynamic Turbulence

Nordita program on “Gravitational Waves from the Early Universe”
Aug. 26 – Sep. 20 2019

Alberto Roper Pol (PhD candidate)

Research Advisor: Axel Brandenburg

Collaborators: Tina Kahniashvili, Arthur Kosowsky, Sayan Mandal

University of Colorado at Boulder

Laboratory for Atmospheric and Space Physics (LASP)

August 26, 2019

1 Introduction and Motivation

2 Gravitational waves

Introduction and Motivation

- Generation of cosmological gravitational waves (GWs) during the electroweak phase transition (EWPT)
- Source of information from earlier times than recombination epoch (Cosmic Microwave Background)

Introduction and Motivation

- Generation of cosmological gravitational waves (GWs) during the electroweak phase transition (EWPT)
- Source of information from earlier times than recombination epoch (Cosmic Microwave Background)
- MHD sources of GWs:
 - Hydrodynamic turbulence from phase transition bubbles nucleation
 - Magnetic turbulence from primordial magnetic fields

Introduction and Motivation

- Generation of cosmological gravitational waves (GWs) during the electroweak phase transition (EWPT)
- Source of information from earlier times than recombination epoch (Cosmic Microwave Background)
- MHD sources of GWs:
 - Hydrodynamic turbulence from phase transition bubbles nucleation
 - Magnetic turbulence from primordial magnetic fields
- Possibility of GWs detection with:
 - Space mission LISA
 - Polarization of CMB
 - Pulsar Timing Arrays (PTA)

Introduction and Motivation

- Generation of cosmological gravitational waves (GWs) during the electroweak phase transition (EWPT)
- Source of information from earlier times than recombination epoch (Cosmic Microwave Background)
- MHD sources of GWs:
 - Hydrodynamic turbulence from phase transition bubbles nucleation
 - Magnetic turbulence from primordial magnetic fields
- Possibility of GWs detection with:
 - Space mission LISA
 - Polarization of CMB
 - Pulsar Timing Arrays (PTA)
- Numerical simulations using `PENCIL CODE` to solve:
 - Relativistic MHD equations
 - Gravitational waves equation

GWs equation for an expanding flat Universe

- Assumptions: isotropic and homogeneous Universe
- Friedmann–Lemaître–Robertson–Walker (FLRW) metric η_{ij}
- Tensor-mode perturbations above the FLRW model:

$$g_{ij} = \eta_{ij} + a^2 h_{ij}^{\text{phys}}$$

- GWs equation is¹

$$(\partial_t^2 - c^2 \nabla^2) h_{ij} = \frac{16\pi G}{ac^2} T_{ij}^{\text{TT}}$$

- h_{ij} are rescaled $h_{ij} = ah_{ij}^{\text{phys}}$
- Comoving spatial coordinates ∇ and conformal time t
- Comoving stress-energy tensor components T_{ij}
- Radiation-dominated epoch such that $a'' = 0$

¹L. P. Grishchuk, *Sov. Phys. JETP*, 40, 409-415 (1974)

Gravitational waves equation

Properties

- Tensor-mode perturbations are gauge invariant
- h_{ij} has only two degrees of freedom: h^+ , h^\times
- The metric tensor is traceless and transverse (TT gauge)

Contributions to the stress-energy tensor

- From fluid motions
$$T_{ij} = (\rho/c^2 + p) \gamma^2 u_i u_j + p \delta_{ij}$$
Relativistic equation of state:
$$p = \rho c^2 / 3$$
- From magnetic fields:
$$T_{ij} = -B_i B_j + \delta_{ij} B^2 / 2$$

Normalized GW equation²

$$\left(\partial_t^2 - \nabla^2\right) h_{ij} = 6 T_{ij}^{\text{TT}} / t$$

Properties

- All variables are normalized and non-dimensional
- Conformal time is normalized with t_*
- Comoving coordinates are normalized with c/H_*
- Stress-energy tensor is normalized with $\mathcal{E}_{\text{rad}}^*$
- Scale factor is $a_* = 1$

²A. Roper Pol et al., *Geophys. Astrophys. Fluid Dyn.*, DOI:10.1080/03091929.2019.1653460, arXiv:1807.05479 (2019) 

Traceless and transverse projection

- For computational reasons, we solve GWs equation sourced by the stress-energy tensor³

$$(\partial_t^2 - c^2 \nabla^2) h_{ij} = \frac{16\pi G}{ac^2} T_{ij}$$

- Projection of h_{ij}^{TT} only at specific times, not at every time-step
- Projection requires Fourier transform \tilde{h}_{ij} (computationally expensive)
- TT projection:

$$\tilde{h}_{ij}^{\text{TT}} = \left(P_{il} P_{jm} - \frac{1}{2} P_{ij} P_{lm} \right) \tilde{h}_{lm}$$

where $P_{ij} = \delta_{ij} - \hat{k}_i \hat{k}_j$

³A. Roper Pol et al., *Geophys. Astrophys. Fluid Dyn.*, DOI:10.1080/03091929.2019.1653460, arXiv:1807.05479 (2019)

Linear polarization modes h^+ and h^\times

Linear polarization basis

$$e_{ij}^+ = (\mathbf{e}_1 \times \mathbf{e}_1 - \mathbf{e}_2 \times \mathbf{e}_2)_{ij}$$

$$e_{ij}^\times = (\mathbf{e}_1 \times \mathbf{e}_2 + \mathbf{e}_2 \times \mathbf{e}_1)_{ij}$$

Orthogonality property

$$e_{ij}^A e_{ij}^B = 2\delta_{AB}, \text{ where } A, B = +, \times$$

h^+ and h^\times modes

$$\tilde{h}^+ = \frac{1}{2} e_{ij}^+ \tilde{h}_{ij}^{\text{TT}}$$

$$\tilde{h}^\times = \frac{1}{2} e_{ij}^\times \tilde{h}_{ij}^{\text{TT}}$$

GWs energy density:

$$\Omega_{\text{GW}}(t) = \mathcal{E}_{\text{GW}} / \mathcal{E}_{\text{rad}}^*, \quad \mathcal{E}_{\text{rad}}^* = \frac{3H_*^2 c^2}{8\pi G}$$

$$\Omega_{\text{GW}}(t) = \int_{-\infty}^{\infty} \Omega_{\text{GW}}(k, t) d \ln k$$

$$\Omega_{\text{GW}}(k, t) = \frac{k}{6H_*^2} \int_{4\pi} \left(|\dot{\tilde{h}}_+^{\text{phys}}|^2 + |\dot{\tilde{h}}_{\times}^{\text{phys}}|^2 \right) k^2 d\Omega_k$$

Antisymmetric GWs energy density:

$$\Xi_{\text{GW}}(t) = \int_{-\infty}^{\infty} \Xi_{\text{GW}}(k, t) d \ln k$$

$$\Xi_{\text{GW}}(k, t) = \frac{k}{6H_*^2} \int_{4\pi} 2\text{Im} \left(\dot{\tilde{h}}_+^{\text{phys}} \dot{\tilde{h}}_{\times}^{\text{phys},*} \right) k^2 d\Omega_k$$

$$H_* \approx 2.066 \cdot 10^{-11} \text{ s}^{-1} \left(\frac{T_*}{100 \text{ GeV}} \right)^2 \left(\frac{g_*}{100} \right)^{1/2}$$

GWs amplitude:

$$h_c(t) = \int_{-\infty}^{\infty} h_c(k, t) d \ln k$$
$$h_c(k, t) = \frac{1}{2} \int_{4\pi} \left(\left| \tilde{h}_+^{\text{phys}} \right|^2 + \left| \tilde{h}_\times^{\text{phys}} \right|^2 \right) k^2 d\Omega_k$$

Numerical results for decaying MHD turbulence⁴

Initial conditions

- Fully helical stochastic magnetic field
- Batchelor spectrum, i.e., $E_M \propto k^4$ for small k
- Kolmogorov spectrum for inertial range, i.e., $E_M \propto k^{-5/3}$
- Total energy density at t_* is $\sim 10\%$ to the radiation energy density⁵
- Spectral peak at $k_M = 100 \cdot 2\pi$, normalized with $k_H = 1/(cH)$

Numerical parameters

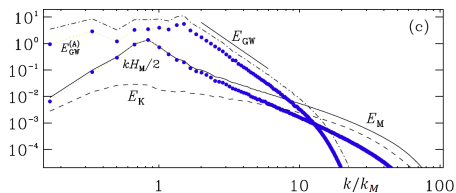
- 1152^3 mesh gridpoints
- 1152 processors
- Wall-clock time of runs is $\sim 1 - 5$ days

⁴A. Roper Pol, *et al.* arXiv:1903.08585

⁵limit from the Big Bang Nucleosynthesis bound

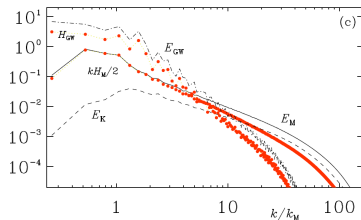
Numerical results for decaying MHD turbulence (old)

Negative initial helicity



$$k_M/k_H = 2$$

Positive initial helicity

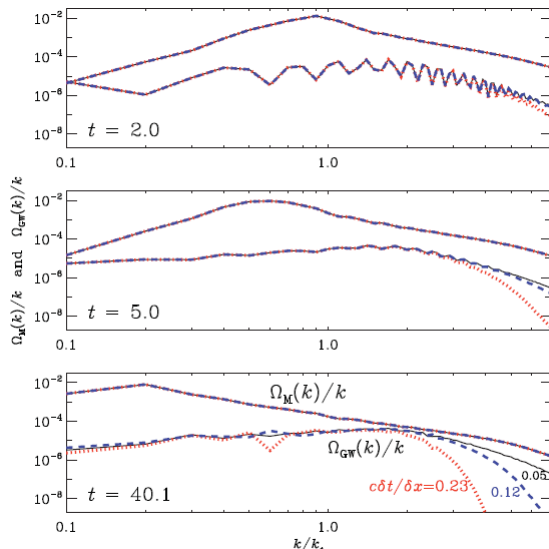


$$k_M/k_H = 6$$

Blue dots indicate negative helicity spectrum (magnetic fields) and negative antisymmetric spectrum (GW)

Red dots indicate positive helicity spectrum (magnetic field) and positive antisymmetric spectrum (GW)

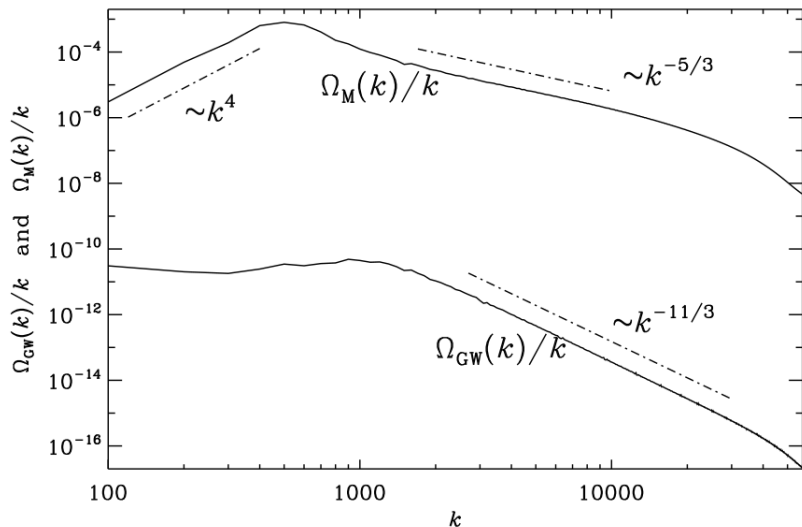
Numerical accuracy⁴



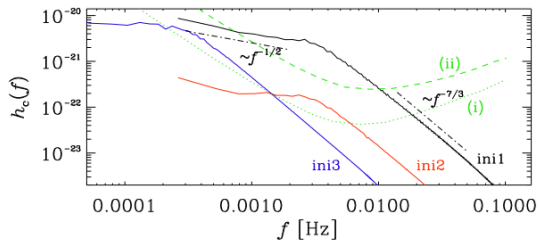
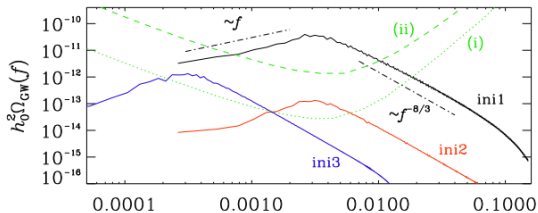
- CFL condition is not enough for GW solution to be numerically accurate
- $c\delta t/\delta x \sim 0.05 \ll 1$
- Higher resolution is required
- Hydromagnetic turbulence does not seem to be affected

⁴ A. Roper Pol et al., *Geophys. Astrophys. Fluid Dyn.*, DOI:10.1080/03091929.2019.1653460, arXiv:1807.05479 (2019)

Numerical results for decaying MHD turbulence



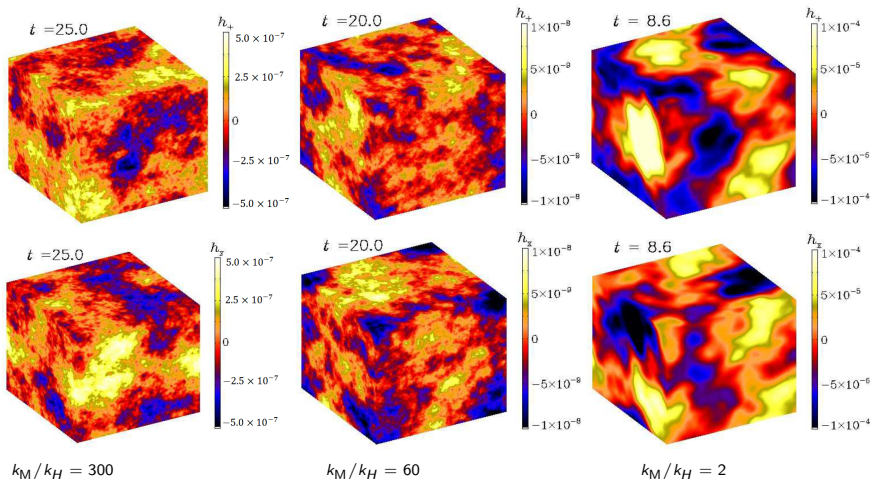
Numerical results for decaying MHD turbulence



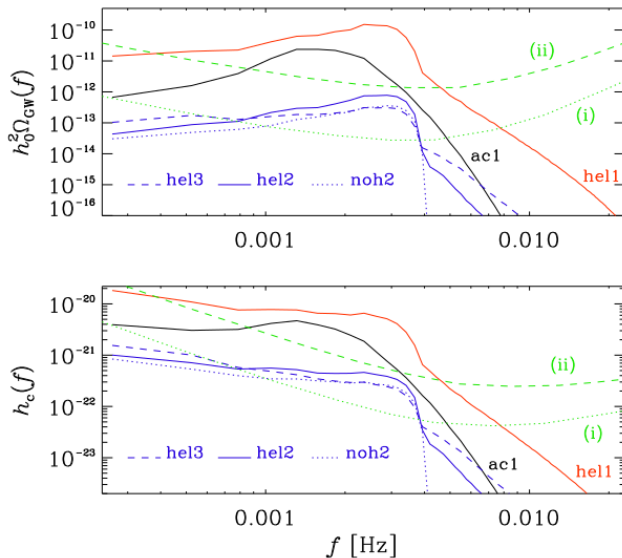
- ini1: $k_M = 100$, $\Omega_M \approx 0.1$
- ini2: $k_M = 100$, $\Omega_M \approx 0.01$
- ini3: $k_M = 10$, $\Omega_M \approx 0.01$

Numerical results for decaying MHD turbulence

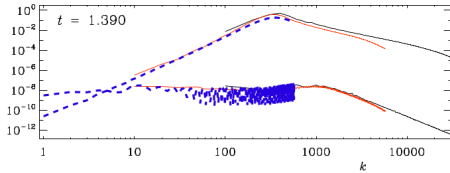
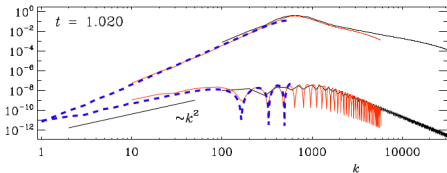
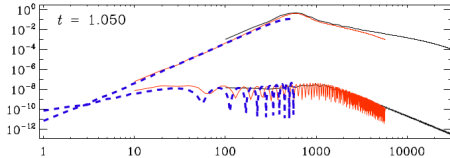
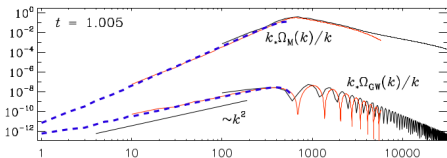
Box results for positive initial helicity:



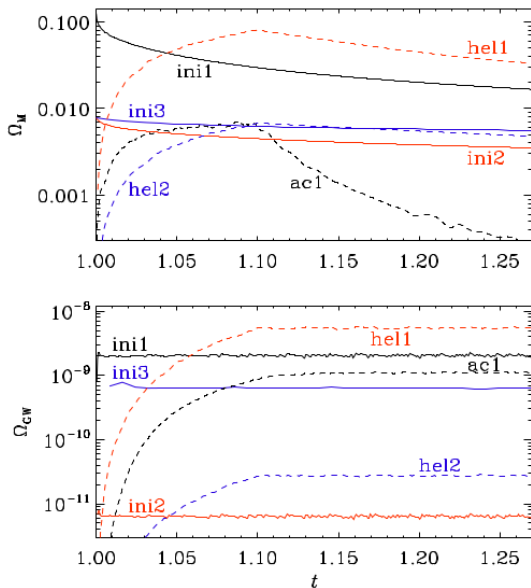
Forced turbulence (built-up primordial magnetic fields and hydrodynamic turbulence), low resolution



Early time evolution of GW energy density spectral slope



Time evolution of GW energy density



Detectability with LISA

LISA

- Laser Interferometer Space Antenna (LISA) is a space based GWs detector
- LISA is planned for 2034
- LISA was approved in 2017 as one of the main research missions of ESA
- LISA is composed by three spacecrafts in a distance of $\sim 2\text{M km}$

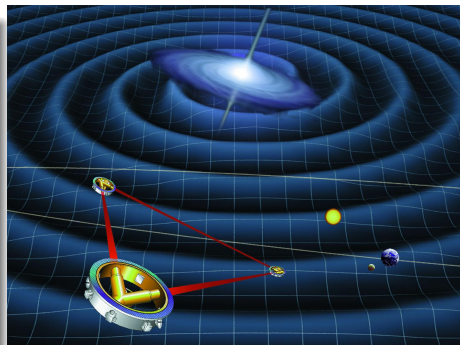


Figure: Artist's impression of LISA from Wikipedia

Detectability with LISA

- LISA sensitivity is usually expressed as $h_0^2 \Omega_{\text{GW}}$
- Ω_{GW} is the ratio of GWs energy density to critical energy density
- Critical energy density is

$$\mathcal{E}_{\text{crit}} = \frac{3H_0^2 c^2}{8\pi G}$$

- Current Hubble parameter is usually expressed as

$$H_0 = 100 h_0 \text{ km s}^{-1} \text{Mpc}^{-1}$$

where h_0 represents the uncertainties in the actual value of H_0

- We consider two different LISA configurations ⁵
 - 4-link configuration with 2×10^9 m arm length after 5 years of duration
 - 6-link configuration with 6×10^9 m arm length after 5 years of duration

⁵C. Caprini et al., JCAP, 2016(04): 001001 (2016)

GW energy density and characteristic amplitude

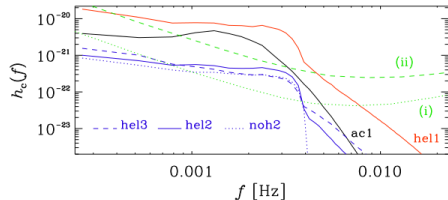
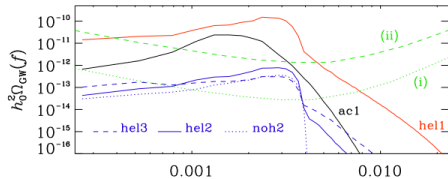
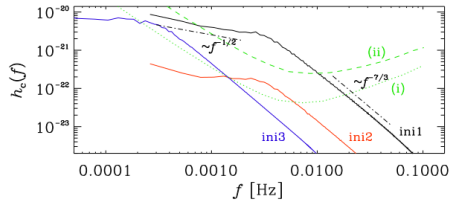
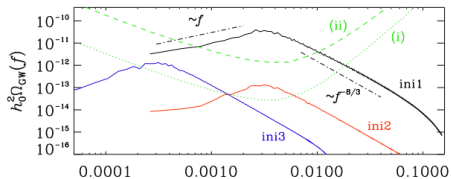
- Shifting due to the expansion of the universe:

- $\Omega_{\text{GW}}^0(k) = a_0^{-4} (H_*/H_0)^2 \Omega_{\text{GW}}(k, t_{\text{end}})$

- $h_c^0(k) = a_0^{-1} h_c(k, t_{\text{end}})$

- $f^0 = a_0^{-1} f$

Detectability with LISA



- We have implemented a module within the `PENCIL CODE` that allows to obtain background stochastic GW spectra from primordial magnetic fields and hydrodynamic turbulence
- For some of our simulations we obtain a detectable signal by future mission LISA
- GW equation is normalized such that it can be easily scaled for different moments within the radiation-dominated epoch
- Bubble nucleation and magnetogenesis physics can be coupled to our equations for more realistic production analysis

The End Thank You!

